

Photochemical Generation of Nitric Oxide from 6-Nitrobenzo[*a*]pyrene

Kiyoshi Fukuhara,* Masaaki Kurihara, and Naoki Miyata*

Contribution from the Division of Organic Chemistry, National Institute of Health Sciences, Setagaya, Tokyo 158-8501, Japan

Received April 9, 2001

Abstract: Photolabile 6-nitrobenzo[*a*]pyrene (6-nitroBaP) released nitric oxide (NO) under visible-light irradiation. The generation of NO and the concomitant formation of the 6-oxyBaP radical were confirmed by ESR. BaP quinones were also detected as further oxidized products of the 6-oxyBaP radical. No such photodegradation was observed with other nitrated BaPs, such as 1-nitroBaP and 3-nitroBaP. DNA-strand breakage, caused by photoexcited 6-nitroBaP, was closely related to its NO-releasing activity. MO calculations of nitrated BaP suggest that the perpendicular conformation of the nitro substituent to the aromatic ring is important for the release of NO with light. These findings may be useful for the development of a new type of NO donor.

Introduction

In this paper, we characterize a nitroarene that can release nitric oxide (NO) and efficiently cleave DNA under photoirradiation. NO has been considered to be an important biological messenger that regulates vasodilation and neurotransmission.¹ It also has important roles as a mediator of the cytotoxic action of macrophages toward tumor cells and microbial pathogens, through the inhibition of mitochondrial enzyme activity and DNA synthesis.² Macrophages also use NO as a cytotoxic agent, which leads to various types of DNA damage.³ It has been shown that NO can deaminate primary amines of DNA under aerobic conditions, and that this leads to mutations and DNA strand breaks.⁴ NO can also react with O₂^{•-} produced from activated macrophages to form peroxynitrate, which is a strong oxidant and nitrating agent, resulting in the modification of protein function⁵ and causing DNA damage.⁶

Attention has been concentrated on the use of caged NO compounds as potent vasodilators in the management of hypertensive

crises and cardiac failure.⁷ This has led to the development of photochemically triggered NO donors, such as metal nitrosyl compounds⁸ and some caged nitric oxides.⁹ The target of NO donors in bioregulation is endothelial cells, and the released NO activates guanyl cyclase. However, little work has been done to develop an NO donor considering cytotoxicity as the major biological outcome.¹⁰ In the present study, we investigated 6-nitrobenzo[*a*]pyrene (6-nitroBaP) (Figure 1) as a potential NO donor and showed that it induces DNA strand breaks upon photoirradiation. Nitrated benzo[*a*]pyrenes (1-, 3-, 6-nitro and 1,6- and 3,6-dinitro) are synthesized by the nitration of benzo[*a*]pyrene (BaP). Among them, 6-nitrated BaPs such as 1,6- and 3,6-dinitro-BaPs are unstable under visible light. The instability of these nitrated BaPs is due to the nitro substituent at the 6-position. We report here that 6-nitroBaP released NO under visible-light irradiation, while no such photodegradation was observed with other nitrated BaPs, such as 1- and 3-nitroBaPs, and that DNA strand breakage was closely related to NO-releasing activity.

Results

To assess the formation of NO upon the photoirradiation of nitroBaPs, an ESR experiment with (MGD)-Fe as the spin trap¹¹ was performed (Figure 2). ESR analysis of 6-nitroBaP photoirradiated for 1 min in the presence of MGD-Fe displayed a three-

* To whom correspondence should be addressed.

(1) Moncada, S.; Palmer, R. M.; Higgs, E. A. *Pharmacol. Rev.* **1991**, *43*, 109–142.

(2) Stuehr, D. J.; Gross, S. S.; Sakuma, I.; Levi, R.; Nathan, C. F. *J. Exp. Med.* **1989**, *169*, 1011–1020.

(3) Hibbs, J. B., Jr.; Taintor, R. R.; Vavrin, Z. *Science* **1987**, *235*, 473–476.

(4) (a) Wink, D. A.; Kasprzak, K. S.; Maragos, C. M.; Elespru, R. K.; Misra, M.; Dunams, T. M.; Cebula, T. A.; Koch, W. H.; Andrews, A. W.; Allen, J. S.; Keefer, L. K. *Science* **1991**, *254*, 1001–1003. (b) Nguyen, T.; Brunson, D.; Crespi, C. L.; Penman, B. W.; Wishnok, J. S.; Tannenbaum, S. R. *Proc. Natl. Acad. Sci. U.S.A.* **1992**, *89*, 3030–3034.

(5) (a) Haddad, I. Y.; Pataki, G.; Hu, P.; Galliani, C.; Beckman, J. S.; Matalon, S. *J. Clin. Invest.* **1994**, *94*, 2407–2413. (b) Kaur, H.; Halliwell, B. *FEBS Lett.* **1994**, *350*, 9–12. (c) Kooy, N. W.; Royall, J. A.; Ye, Y. Z.; Kelly, D. R.; Beckman, J. S. *Am. J. Respir. Crit. Care Med.* **1995**, *151*, 1250–1254.

(6) (a) King, P. A.; Anderson, V. E.; Edwards, J. O.; Gustafson, G.; Plumb, R. C.; Suggs, J. W. *J. Am. Chem. Soc.* **1992**, *114*, 5430–5432. (b) Salgo, M. G.; Stone, K.; Squadrito, G. L.; Battista, J. R.; Pryor, W. A. *Biochem. Biophys. Res. Commun.* **1995**, *210*, 1025–1030. (c) Rubio, J.; Yermilov, V.; Ohshima, H. In *The Biology of Nitric Oxide*; Moncada, S., Stamler, J., Gross, S., Higgs, E. A., Eds.; Portland Press Proceedings: London, England, 1996; p 34. (d) Tamir, S.; Burney, S.; Tannenbaum, S. R. *Chem. Res. Toxicol.* **1996**, *9*, 821–827.

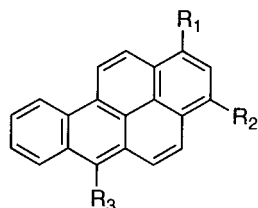
(7) (a) Bisset, W. I. K.; Burdon, M. G.; Butler, A. R.; Glidewell, C.; Reglinski, J. *J. Chem. Res., Synop.* **1981**, 299. (b) Clarke, M. J.; Gaul, J. B. *Struct. Bonding* **1993**, *81*, 147–181.

(8) Flitney, F. W.; Megson, I. L.; Flitney, D. E.; Butler, A. R. *Br. J. Pharmacol.* **1992**, *107*, 842–848.

(9) (a) Makings, L. R.; Tsien, R. Y. *J. Biol. Chem.* **1994**, *269*, 6282–6285. (b) Kwon, N. S.; Lee, S. H.; Choi, C. S.; Kho, T.; Lee, H. S. *FASEB J.* **1994**, *8*, 529–533. (c) Singh, R. J.; Hogg, N.; Joseph, J.; Kalyanaraman, B. *FEBS Lett.* **1995**, *360*, 47–51. (d) Namiki, S.; Kaneda, F.; Ikegami, M.; Arai, T.; Fujimori, K.; Asada, S.; Hama, H.; Kasuya, Y.; Goto, K. *Bioorg. Med. Chem.* **1999**, *7*, 1695–1702.

(10) Hou, Y.; Wang, J.; Andreana, P. R.; Cantauria, G.; Tarasia, S.; Sharp, L.; Braunschweiger, P. G.; Wang, P. G. *Bioorg. Med. Chem. Lett.* **1999**, *9*, 2255–2258.

(11) Komarov, A.; Mattson, D.; Jones, M. M.; Singh, P. K.; Lai, C.-S. *Biochem. Biophys. Res. Commun.* **1993**, *195*, 1191–1198.



1-nitroBaP: $R_1=NO_2$, $R_2=R_3=H$
 3-nitroBaP: $R_2=NO_2$, $R_1=R_3=H$
 6-nitroBaP: $R_3=NO_2$, $R_1=R_2=H$

Figure 1. Structures of 1-, 3- and 6-nitroBaPs.

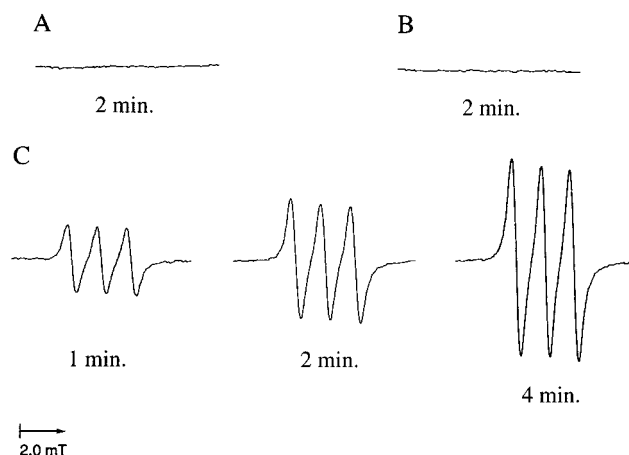


Figure 2. ESR spectra of Fe-MGD in the presence of 1-, 3-, and 6-nitroBaPs. Samples contained 200 μM of 1-nitroBaP (A), 3-nitroBaP (B), or 6-nitroBaP (C), 75 mM of MGD, and 15 mM of $FeSO_4$ in phosphate buffer at pH 7.2 (containing 20% DMF); ESR spectra were recorded after photoirradiation for 1, 2, and 4 min (6-nitroBaP) or 2 min (1- and 3-nitroBaPs), with a modulation amplitude of 2.0 G.

line spectrum consisting of $a^N = 1.25$ mT and $g^{iso} = 2.04$, which is characteristic of the $[(MGD)_2-Fe^{2+}-NO]$ complex. An increase in the signal intensity of the $[(MGD)_2-Fe^{2+}-NO]$ adduct was observed with an increase in the duration of irradiation, indicating the photolytic generation of NO from 6-nitroBaP. When similar experiments were performed with 1- and 3-nitroBaPs, no ESR signals were detected.

CarboxyPTIO was also used to detect NO¹² to further confirm the production of NO via the photolysis of 6-nitroBaP (Figure 3). The ESR signal of carboxyPTIO is characterized by five lines (1:2:3:2:1, $a^N = 0.82$ mT). If NO is oxidized by carboxyPTIO, the latter is transformed to carboxyPTI, which has seven line signals on ESR ($a^{N1} = 0.92$ mT, $a^{N2} = 0.54$ mT). After photoirradiation of a mixture of 6-nitroBaP and carboxyPTIO, a time-dependent decrease in signals for carboxyPTIO was observed, concomitant with an increase in signals for carboxyPTI, indicating the production of NO from 6-nitroBaP. The transformation of carboxyPTIO to carboxyPTI was not observed if a solution of carboxyPTIO was irradiated in the presence of 1- or 3-nitroBaP (data not shown).

ESR spectroscopy was also used to assess the radical that was produced as a result of the release of NO from photoirradiated 6-nitroBaP (Figure 4). Photoirradiation of 6-nitroBaP resulted in the appearance of an ESR signal composed of five lines (1:4:6:4:1), consistent with unpaired electrons interacting with four protons, the amplitude of which increased with the

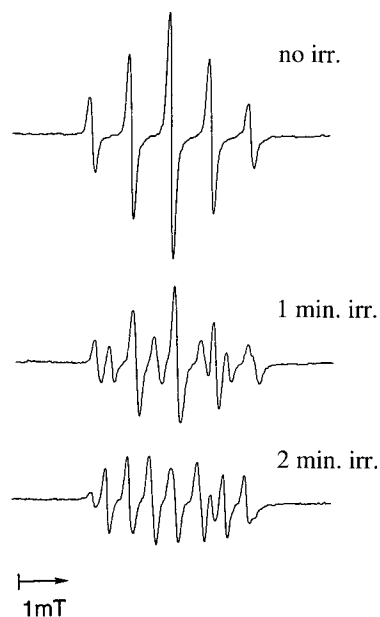


Figure 3. ESR spectra of carboxyPTIO in the presence of 6-nitroBaP. Samples contained 5 μM carboxyPTIO and 200 μM 6-nitroBaP in phosphate buffer at pH 7.6 (containing 20% DMF); ESR spectra were recorded with a modulation amplitude of 2.0 G after photoirradiation for 0, 1, or 2 min.

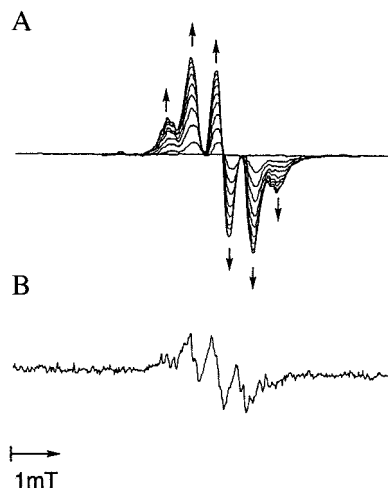


Figure 4. ESR spectra of 6-nitroBaP under photoirradiation: (A) 200 μM of 6-nitroBaP in phosphate buffer at pH 7.6 (containing 20% DMF) was photoirradiated for 0, 0.5, 2, 4, 6, 8, 10, 12, or 16 min, with ESR spectra at a modulation amplitude of 2.0 G were recorded under photoirradiated conditions; (B) ESR spectra of 6-nitroBaP photoirradiated for 5 min recorded at a modulation amplitude of 0.2 G.

duration of irradiation. Each of the four lines was further resolved into more protons when the spectrum was recorded at a lower modulation amplitude, indicating interactions with additional protons. Based on comparison of these signals with those published in the literature,^{13,14} we unambiguously concluded that the 6-oxyBaP radical is formed with the release of NO upon photoirradiation of 6-nitroBaP.

Inomata and Nagata demonstrated that the 6-oxyBaP radical produced from photoirradiated BaP afforded further oxidation, resulting in the formation of BaP quinones.¹³ To investigate the nature of the 6-oxyBaP radical formed upon irradiation of 6-nitroBaP, we monitored the photochemical reaction products

(12) Akaike, T.; Yoshida, M.; Miyamoto, Y.; Sato, K.; Kohno, M.; Sasamoto, K.; Miyazaki, K.; Ueda, S.; Maeda, H. *Biochemistry* **1993**, *32*, 827–832.

(13) Inomata, M.; Nagata, C. *Gann* **1972**, *63*, 119–130.

(14) Lorentzen, R. J.; Lesko, S. A.; McDonald, K.; Ts'ao, P. O. *Biochemistry* **1975**, *14*, 3970–3977.

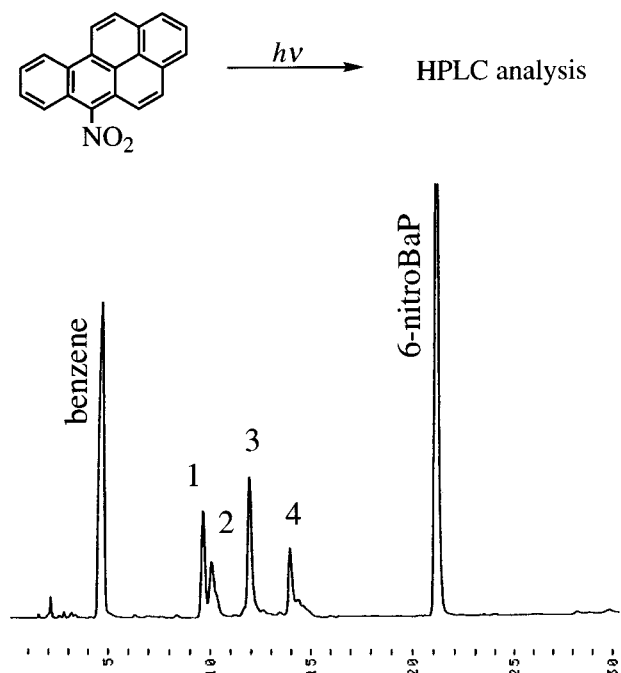


Figure 5. HPLC profile of the products formed from photoirradiated 6-nitroBaP. For analysis conditions, see the Experimental Section. The peak at 4.5 min represents benzene as the solvent. The numbers above the peaks correspond to (1) 1,6-BaPQ, (2) 3,6-BaPQ, (3) 6,12-BaPQ, and (4) 6-OHBaP.

Table 1. Yields of the Products Formed from Photoirradiated 6-nitroBaP

reaction time, h	products (%)				
	1,6-BQ	3,6-BQ	6,12-BQ	6-OHBQ	6-nitroBaP
1	4.6	3.0	7.1	6.7	74.0
2	9.8	8.4	16.8	10.6	46.9
1 ^a	1.4	0.8	2.8	14.5	70.6

^a Reaction was run under argon.

by HPLC. Irradiation of 6-nitroBaP solution for 1 h resulted in four major peaks (Figure 5). The peaks on the HPLC profile corresponded to 6-OHBaP (6.7% yield) and 1,6-, 3,6-, and 6,12-BaP quinones (4.6, 3.0, and 7.1% yield), respectively, the yields of which increased with the duration of irradiation. When the photolysis of 6-nitroBaP was performed under argon, a decrease in the yield of BaP quinones and an increase in that of 6-OHBaP were observed (Table 1), suggesting that BaP quinones are formed as a result of the oxidation of 6-oxyBaP radical by molecular oxygen. Although 6-OHBaP can be oxidized to form BaP quinones, the rate of the reaction is relatively slow under the conditions used for the photolysis of 6-nitroBaP (data not shown). Therefore, the major participation of 6-OHBaP, derived from the 6-oxyBaP radical, in the production of BaP quinones by photooxidation can be ruled out.

In the presence of oxygen, NO causes the deamination of purines and pyrimidines and the oxidation of purines to give several types of mutation.¹⁵ Deamination of bases by oxidized NO also leads to the production of abasic sites and subsequent single-strand breaks. Sugiura and Matsumoto investigated the direct DNA damage caused by NO and demonstrated that NO caused single-strand breaks with preferential cleavage at G.¹⁶ To determine if the photoinduction of NO from 6-nitroBaP can

cause DNA strand breaks, 1-, 3-, and 6-nitroBaPs at a concentration of 50 μ M were mixed with supercoiled plasmid pBR322 and photoirradiated (Figure 6). When irradiation was performed for 30 min, 6-nitroBaP effected the conversion of Form I (supercoiled) DNA to Form II (relaxed circular) DNA. Quantitative and significant conversion of Form I to Form II DNA was observed with 6-nitroBaP by increasing the duration of irradiation, while less-efficient DNA cleavage resulted when 1- and 3-nitroBaPs were used. The efficiency of 6-nitroBaP in DNA cleavage depended on the duration of irradiation, and 6-nitroBaP failed to effect plasmid DNA relaxation when the reaction was performed in the presence of carboxyPTIO to trap photoreleased NO, suggesting that NO was responsible for the observed DNA damage mediated by photoirradiated 6-nitroBaP (see Supporting Information). In addition to efficient DNA cleavage by 6-nitroBaP, Form I DNA showed reduced gel mobility. No such shift resulted with 1- and 3-nitroBaPs, and 6-nitroBaP did not affect gel mobility without irradiation (see Supporting Information). A shift in gel mobility is caused by unwinding of the phosphodiester backbone to accommodate an intercalater.¹⁷ Therefore, a slower band might be due to the strong intercalation into supercoiled DNA of photoirradiated products, BaP quinones, rather than 6-nitroBaP itself.

Discussion

The present study demonstrated that photoirradiated 6-nitroBaP is capable of giving rise to NO and causing DNA strand scission. Photoirradiated production of NO is characteristic of 6-nitroBaP. No such irradiation-dependent release of NO and induction of DNA cleavage was seen with 1- and 3-nitroBaPs. In the photoirradiated production of NO by 6-nitroBaP, the formation of 6-oxyBaP radical suggested that NO was generated via 6-nitriteBaP, which was produced from 6-nitroBaP by an intramolecular rearrangement mechanism (Figure 7). The mechanism, where 6-oxyBaP radical is directly derived from 6-nitriteBaP as an intermediate via homolytic cleavage of the N–O bond, may also be evidenced by the photoinduced formation of 6-OHBaP. In fact, the yield of 6-OHBaP was improved under anaerobic conditions.

Semiempirical MO calculations were performed to assess which characteristic of the structure is responsible for NO generation (Table 2), where the plane of the nitro group was perpendicular to the aromatic ring of 6-nitroBaP, while the dihedral angle for 1- and 3-nitroBaPs was about 60°. This suggests that the overlap of the half-vacant nonbonding orbital of the nitro group at the 6-position with the adjacent orbital of the aromatic ring increases susceptibility to intramolecular rearrangement from the nitro to nitrite. In comparison, such intramolecular rearrangement does not occur in the case of 1- and 3-nitroBaPs, which do not generate NO, since the dihedral angle between the plane of the nitro and aromatic ring is unfavorable for the overlap of the orbitals in the excited state. The differences (ΔE) in the heat of formation between nitro and nitrite were also estimated by semiempirical MO calculation. The fact that 6-nitroBaP has the lowest ΔE among these compounds provides further evidence that NO is generated via a mechanism of nitro-to-nitrite rearrangement. NO production has also been observed in the photochemical oxidation of 9-nitroanthracene.¹⁸ However, the ability to provide NO was

(15) Caulfield, J. L.; Wishnok, J. S.; Tannenbaum, S. R. *J. Biol. Chem.* **1998**, *273*, 12689–12695.

(16) Sugiura, Y.; Matsumoto, T. *Biochem. Biophys. Res. Commun.* **1995**, *211*, 748–753.

(17) (a) Islam, S. A.; Neidle, S.; Gandecha, B. M.; Brown, J. R. *Biochem. Pharmacol.* **1983**, *32*, 2801–2808. (b) Zeman, S. M.; Depew, K. N.; Danishefsky, S. M.; Crothers, D. M. *Proc. Natl. Acad. Sci. U.S.A.* **1998**, *95*, 4327–4332.

(18) Chapman, O. L.; Heckert, D. C.; Reasoner, J. W.; Thackaberry, S. P. *J. Am. Chem. Soc.* **1966**, *88*, 5550–5554.

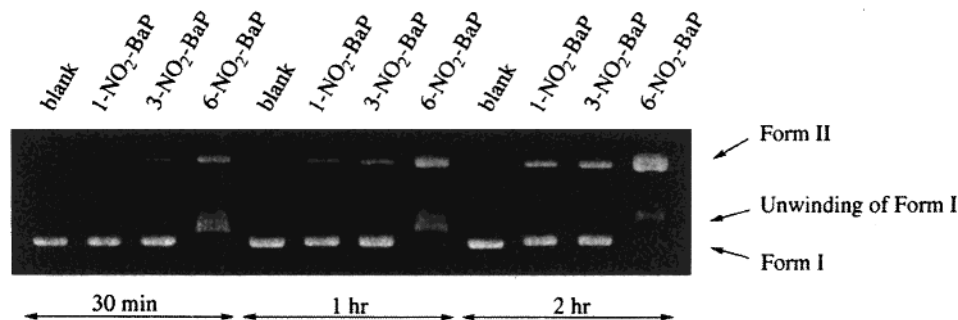


Figure 6. Cleavage of supercoiled pBR322DNA by 1-, 3-, and 6-nitroBaPs upon photoirradiation.

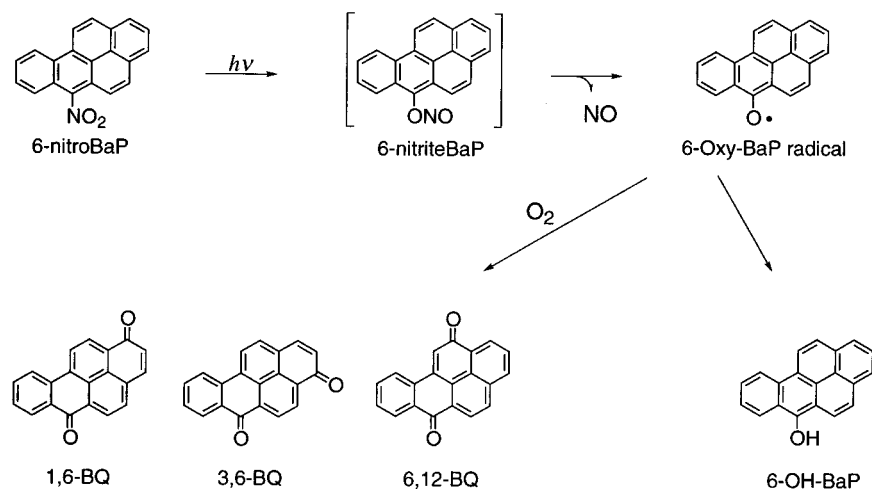


Figure 7. Predicted pathway for the photochemical reaction of 6-nitroBaP with the generation of NO from the nitro group.

Table 2. Results of Semiempirical MO Calculations

comps	dihedral angle ^a	ΔE^b
nitrobenzene	3	10.89
9-nitroanthracene	88	8.54
1-nitroBaP	58	9.04
3-nitroBaP	59	9.08
6-nitroBaP	90	6.73

^a Dihedral angle (deg) between the planes of the nitro group and the aromatic moiety. ^b Difference (kcal mol⁻¹) in heat of formation (HF) between the nitro (R-NO₂) and nitrite (R-ONO) forms: $\Delta E = (\text{HF of R-ONO}) - (\text{HF of R-NO}_2)$.

very much weaker than that with 6-nitroBaP (data not shown) despite the same dihedral angle (88°). The smaller ΔE of 6-nitroBaP compared to that of 9-nitroanthracene might account for the predominance of 6-nitroBaP for NO generation.

While both 1- and 3-nitroBaP have been shown to exhibit a variety of biological activities, including bacterial and mammalian mutagenicity,¹⁹ and cell toxicity, no such activities have been shown by 6-nitroBaP.²⁰ Enzymatic reduction of the nitro group to an activated form and subsequent DNA-adduct formation is responsible for the mutagenicity of 1- and 3-nitroBaP. On the other hand, such reductive activation cannot occur with 6-nitroBaP, since two peri protons at the 5- and 7-positions impede the access of reductase to 6-nitroBaP,²¹ suggesting that the nitro group at the 6-position of BaP is insensitive to enzymatic reduction. Although BaP is a potent

(19) Pitts, J. N., Jr.; Zielinska, B.; Harger, W. P. *Mut. Res.* **1984**, *140*, 81–85.

(20) Chou, M. W.; Heflich, R. H.; Casciano, D. A.; Miller, D. W.; Freeman, J. P.; Evans, F. E.; Fu, P. P. *J. Med. Chem.* **1984**, *27*, 1156–1161.

(21) Pitts, J. N., Jr.; Lokensgard, D. M.; Harger, W.; Fisher, T. S.; Mejia, V.; Schuler, J. J.; Scorziell, G. M.; Katzenstein, Y. A. *Mut. Res.* **1982**, *103*, 241–249.

mutagenic and carcinogenic compound, nitrated BaPs have not been shown to exhibit biological activities by the same mechanism as BaP.²² The electron deficiency of the BaP ring due to the inducing effect of the nitro group hinders metabolic oxidation, as in the case with BaP, whose oxidative metabolites are responsible for mutagenicity and carcinogenicity. Therefore, the finding that 6-nitroBaP is a photodependent DNA-damaging agent may be useful for the development of a new type of NO donor.

Experimental Section

Materials. The 1-, 3-, and 6-nitroBaPs were synthesized by nitration of BaP.²³ MGD and carboxyPTIO were purchased from DOJINDO and pBR322 DNA was purchased from Nippon Gene. All other chemicals and solvents were reagent grade or better. In all experiments, irradiation was performed through a Pyrex filter with a 300-W photoreflexor lamp.

ESR Analysis. The Fe²⁺ complex of MGD [Fe²⁺-MGD₂, (Fe-MGD)] was used to trap NO. Fresh stock solutions of Fe-MGD (1:5) were prepared by adding ferrous ammonium sulfate to an aqueous solution of MGD. CarboxyPTIO was also used for NO detection. A sample containing 200 μM nitroBaP and 15 mM MGD-Fe or 5 μM carboxyPTIO in phosphate buffer at pH 7.6 (25% DMF) was introduced into a quartz flat cell. ESR spectra were recorded after light irradiation at a distance of 30 cm with a JES-FE 2XG spectrometer (JEOL Co. Ltd., Tokyo, Japan). To measure the 6-oxyBaP radical, photolysis of a sample containing 200 μM 6-nitroBaP in phosphate buffer at pH 7.6 (25% DMF) was performed by using light irradiation focused in a 1-cm-diameter beam on the ESR flat cell that was placed in the cavity with the front plate removed. The spectrometer settings were modulation frequency, 100 kHz; modulation amplitude, 2G or 0.2G; scan time, 4 min; microwave power, 16 mW; and microwave frequency, 9.394 GHz.

(22) Fu, P. P. *Drug Metab. Rev.* **1990**, *22*, 209–268.

(23) Fukuhara, K.; Miyata, N.; Matsui, M.; Matsui, K.; Ishidate, M., Jr.; Kamiya, S. *Chem. Pharm. Bull.* **1990**, *38*, 3158–3161.

Analysis of Photoirradiation Products. To analyze photoirradiation products of 6-nitroBaP, 10 mM 6-nitroBaP in 10 mL of benzene was irradiated (at a distance of 20 cm) at 37 °C. The progress of the reaction was monitored by HPLC on a Shimadzu HPLC system. Aliquots of the reaction mixture were loaded onto a Senshu Pegasil C18 column (5 μ ; 100 \times 4.6), eluted at 1 mL/min with a linear gradient from 30:70 (vol/vol) 0.1 M NH₄HCO₃ buffer at pH 7.0:methanol to 100% methanol over 30 min. After irradiation for 2 h, the reaction mixture was concentrated by rotary evaporation and purified by semipreparative HPLC on a Wakosil-II 5C18 AR (5 μ m; 300 \times 10) with the same gradient and solvents that were used to monitor the reaction and a flow rate of 10 mL/min. The product fractions corresponding to peaks for 1,6-, 3,6-, and 6,12-benzo[*a*]pyrenequinone (BaPQ) and 6-OH-BaP were collected, concentrated by rotary evaporation, and dried in vacuo. 1,6-BaPQ: 9.8% yield; ¹HNMR (CDCl₃) δ 6.77 (d, *J* = 10.0, H₂), 7.63 (m, H₈), 7.73 (d, *J* = 10.0, H₃), 7.79 (m, H₉), 7.90 (d, *J* = 7.2, H₄), 8.34 (d, *J* = 8.1, H₁₀), 8.46 (d, *J* = 7.6, H₇), 8.56 (d, *J* = 7.8, H₁₁), 8.63 (d, *J* = 7.8, H₁₂), 8.67 (d, *J* = 7.2, H₅). 3,6-BaPQ: 8.4% yield; ¹HNMR (CDCl₃) δ 6.74 (d, *J* = 9.7, H₂), 7.62 (m, H₈), 7.76 (d, *J* = 9.7, H₁), 7.79 (m, H₉), 7.83 (d, *J* = 7.6, H₁₂), 8.31 (d, *J* = 7.8, H₁₀), 8.41 (d, *J* = 7.6, H₁₁), 8.48 (d, *J* = 7.8, H₇), 8.76 (d, *J* = 7.4, H₅), 8.86 (d, *J* = 7.4, H₄). 6,12-BaPQ: 16.8% yield; ¹HNMR (CDCl₃) δ 7.59 (s, H₁₁), 7.69 (m, H₈), 7.79 (m, H₉), 7.86 (dd, *J* = 7.1 and 8.4, H₂), 8.18 (d, *J* = 8.5, H₄), 8.21 (d, *J* = 8.2, H₁₀), 8.24 (d, *J* = 8.4, H₃), 8.46 (d, *J* = 7.4, H₇), 8.48 (d, *J* = 8.5, H₅), 8.64 (d, *J* = 7.1, H₁). 6-OH-BaP: 10.6% yield; ¹HNMR (CDCl₃) δ 7.80 (m, H₉), 7.82 (m, H₈), 7.92 and 7.93 (d, *J* = 9.6, H₄ and H₅), 7.95 (dd, *J* = 7.6 and 8.8, H₂), 8.05 (d, *J* = 7.6, H₃), 8.20 (d, *J* = 8.8, H₁), 8.23 (d, *J* = 8.8, H₇), 8.25 (d, *J* = 9.0, H₁₂), 8.95 (d, *J* = 9.2, H₁₁), 9.02 (d, *J* = 7.2, H₁₀). The structures

of 1,6-, 3,6-, and 6,12-BaPQ and 6-OH-BaP were also confirmed by comparison with authentic standards, synthesized according to reported procedures.²⁴

Assays for DNA Strand Breaks. DNA strand breakage was measured by the conversion of supercoiled pBR322 plasmid DNA to the open circular form. Reactions were carried out in 20 μ L (total volume) of 50 mM Na cacodylate buffer (20% DMF), pH 7.2, containing 45 μ M pBR322 DNA and 50 μ M nitroBaPs. The reaction mixtures were irradiated (at a distance of 30 cm) at 0 °C for an appropriate time and then treated with 5 μ L of loading buffer (100 mM TBE buffer, pH 8.3, containing 30% glycerol, 0.1% bromophenol blue) and applied to 1% agarose gel. Horizontal gel electrophoresis was carried out in 50 mM TBE buffer, pH 8.3, and the gels were stained with ethidium bromide (1 μ g/mL) for 30 min, followed by destaining in water for 30 min and photography with UV transillumination.

Semiempirical MO Calculations. Semiempirical MO calculations were performed with SPARTAN (ver. 3.1, Wavefunction Inc.). All structures were fully optimized at the restricted Hartree–Fock level with the PM3 method.

Supporting Information Available: Figure 1s showing the effect of carboxyPTIO on photoirradiated reaction, and Figure 2s showing the effect of nitroBaPs on pBR322DNA in the dark (PDF). This material is available free of charge via the Internet at <http://pubs.acs.org>.

JA0109038

(24) (a) Fieser, L. F.; Hershberg, E. B. *J. Am. Chem. Soc.* **1938**, *60*, 2542–2548. (b) Lee-Ruff, E.; Kazarians-Moghaddam, H.; Katz, M. *Can. J. Chem.* **1986**, *64*, 1297–1303.